

©2017

Jingjing Shi

ALL RIGHTS RESERVED

STUDY OF TOP2B FUNCTION ON FIBROBLAST MIGRATION USING  
MICROFLUIDIC DEVICE

By

Jingjing Shi

A thesis submitted to the

Graduate School-New Brunswick

Rutgers, The State University of New Jersey

In partial fulfillment of the requirements

For the degree of

Master of Science

Graduate Program in Biomedical Engineering

Written under the direction of

Li Cai, Ph.D.

And approved by

---

---

---

---

New Brunswick, New Jersey

October 2017

ABSTRACT OF THE THESIS  
STUDY OF TOP2B FUNCTION ON FIBROBLAST MIGRATION USING  
MICROFLUIDIC DEVICE

by JINGJING SHI

Thesis Director:

Li Cai, Ph.D.

**Background:** Top2b is known to be essential in neural development. The lack of Top2b in embryonic stem cell (ESC)-derived neurons may cause premature cell death, as well as abnormal retinal development. So far, few research has focused on using fibroblasts to investigate the function of Top2b. Therefore, function of Top2b in fibroblast migration still remains unclear.

**Material and methods:** Fibroblasts were obtained from postnatal day 1 (P1) mice and cultured for 7 days before transferred to microfluidic devices. Top2b inhibitor ICRF-193 was used to suppress Top2b function and determine the effect of Top2b on fibroblast migration. Fibroblasts were seeded on one side of two-chamber microfluidic devices and treated with 0.1  $\mu$ M, 1  $\mu$ M, and 10  $\mu$ M ICRF-193, whereas equal concentration of DMSO and DMEM were used as controls. Continuous 7-day observation starts from 1 day after seeding cells on devices. Overnight time-lapse microscopy was performed on cells between 2 days and 4 days.

**Results:** Significant differences in the number and speed of fibroblast cell migration were observed with ICRF-193 treatment. Higher concentration of ICRF-193 resulted in fewer cells in the migration chamber and slower migration speed.

**Conclusions:** These results demonstrate an important role of Top2b in fibroblast migration, thus further making Top2b as a potential target for wound healing and treatment of cancer.

## ACKNOWLEDGEMENTS

First, I would like to convey my gratefulness to my advisor, Dr. Li Cai, for providing me the opportunity to be a member in Cai Lab. I cannot complete my research study and thesis without his patient guidance and constant encouragement.

Also, I would like to thank my committee members, Dr. Jay C. Sy and Dr. Jeffrey D. Zahn, for their support, advice, and constructive criticism on my thesis. I would also like to provide a special thank you to Dr. Zahn for providing use of his equipment and materials for my research.

I am grateful for having a chance to work with all the current members in Cai Lab. I want to thank Jeremy Anderson, Misaal Patel, Dr. Ying Li, and Rameshwari Rayaji for giving me advice in research and thesis, as well as giving me help on various new techniques during my time in lab.

I would also like to thank Joseph Fantuzzo for his guidance on making microfluidic devices and a thank you to Xin Liu and Ruixiao Li for helping me on using engineering software.

Last but not the least, I would like to express the deepest appreciation to my parents who not only provide me financial support, but also give me constant encouragement for all through this time.

## TABLE OF CONTENTS

ABSTRACT .....	ii
ACKNOWLEDGEMENTS .....	iv
TABLE OF CONTENTS .....	v
LIST OF FIGURES .....	vii
LIST OF ABBREVIATIONS .....	viii
CHAPTER I BACKGROUND AND SIGNIFICANCE	
1.1 Cell migration .....	1
1.1.1 Fibroblasts and fibroblast migration .....	4
1.2 Function of Top2b .....	5
1.2.1 Top2b inhibitor ICRF-193 .....	9
1.3 Microfluidic device .....	12
1.4 Rationale .....	13
CHAPTER II MATERIALS AND METHODS	
2.1 Design and fabrication .....	15
2.2 Animals and isolation of mouse primary fibroblasts .....	18
2.3 Device sterilization and cell loading .....	18
2.4 Treatment with Top2b inhibitor ICRF-193.....	19
2.5 Imaging .....	19
2.6 Time-lapse microscopy .....	19
2.7 Data analysis .....	20
CHAPTER III RESULTS	
3.1 Microfluidic device is an excellent system for cell migration study.....	21

3.2 Fibroblasts migrate into and through microchannel structures -----	24
3.3 Top2b inhibition by ICRF-193 suppresses fibroblast migration -----	25
3.4 Top2b inhibition by ICRF-193 suppresses fibroblast movement -----	29
CHAPTER IV DISCUSSION	
4. Discussion -----	32
REFERENCES -----	36

## **LIST OF FIGURES**

### **CHAPTER 1**

Figure 1.1 Basic mechanism of cell movement

Figure 1.2.1 Function of Top2b

Figure 1.2.2 Inhibition effect of ICRF-193 on Top2b

### **CHAPTER 2**

Figure 2.1 Two kinds of microfluidic devices

### **CHAPTER 3**

Figure 3.1.1 Cell culture in microfluidic devices

Figure 3.1.2 Number of cells in the migration chamber

Figure 3.2.1 Fibroblasts migrate through microchannels

Figure 3.3.1 Top2b inhibition by ICRF-193 reduces fibroblast cell migration

Figure 3.3.2 Statistical analysis of fibroblast cell migration under Top2b inhibition by ICRF-193

Figure 3.4.1 Top2b inhibition by ICRF-193 decreases the speed of fibroblast migration

Figure 3.4.2 Statistical analysis of the speed of fibroblast cell migration under Top2b inhibition by ICRF-193



## LIST OF ABBREVIATIONS

ANOVA	Analysis of Variance
ATP	Adenosine triphosphate
BER	Base excision repair
CAFs	Cancer-associated fibroblasts
CNS	Central nervous system
DI	Deionized
DMEM	Dulbecco's Modified Eagle's Medium
DMSO	Dimethyl sulfoxide
DSB	Double-strand break
ECM	Extracellular matrix
EDTA	Ethylenediaminetetraacetic acid
ESC	Embryonic stem cell
FBS	Fetal bovine serum
FGFs	Fibroblast growth factors
HIV	Human immunodeficiency virus

IACUC	the Institutional Animal Care and Use Committee
IPA	Isopropyl alcohol
NGF	Nerve growth factor
PBS	Phosphate buffered saline
PDMS	Polydimethylsiloxane
PLEKHG3	Pleckstrin homology and RhoGEF domain containing G3
PIP3	Phosphatidylinositol triphosphate
PTEN	Phosphatase and tensin homolog
SCF	Stem cell factor
SUMO	Small ubiquitin-like modifier
Top2a	Topoisomerase II alpha
Top2b	Topoisomerase II beta
VM	Ventral mesencephalic

## **CHAPTER I BACKGROUND AND SIGNIFICANCE**

This study uses microfluidic devices to explore the function of Top2b on fibroblast cell migration. In this chapter, background of cell migration, fibroblasts, the role of Top2b, and microfluidic devices will be introduced. The significance of conducting this research will also be discussed.

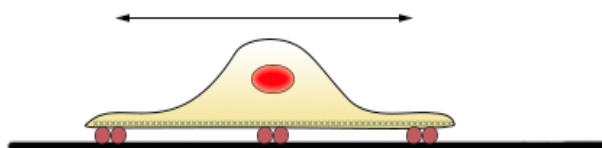
### ***1.1 Cell migration***

Cell migration is the process through which cells move from one location to another by using various motility methods. It is an essential process for all organisms to develop and maintain their basic functions. For example, wound healing, immune surveillance and embryonic development all rely on cell migration to maintain healthy bodily function. So far, the basic mechanism of cell motility has been well understood (Petrie et al., 2009). During cell movement, first the cell determines its leading and rear sides and forms a protrusion from the leading side by actin polymerization. Then, the cell adheres the leading side to the substrate. Lastly, the cell releases its rear side and the whole cell body contracts through cytoskeleton actin/myosin II contraction. This force pulls the cell body forward (Figure 1.1) (Ananthakrishnan and Ehrlicher, 2007). During the polarization process, some cells, such as Dictyostelium and some immune cells, form their leading sides due to an external agent. For instance, since the polarization of phosphatase and tensin homolog (PTEN), a lipid phosphatase, phosphatidylinositol triphosphate (PIP3) is produced at the leading edge and

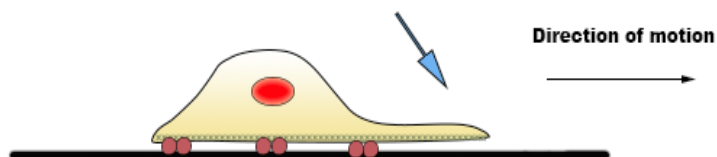
contributes to polarity. Also, the small GTPase Cdc42 and signaling molecules like PKC are able to facilitate polarity. In some cells the rear sides are established by the contractile protein, such as myosin II, that produces huge amount of actomyosin filaments and adhesions (Petrie et al., 2009). In addition, recent research has found that the pleckstrin homology and RhoGEF domain containing G3 (PLEKHG3) can selectively binds to new-formed polymerized actin at the leading edge of migrating fibroblasts and thus positively regulate cell migration (Nguyen et al., 2016).

Research has investigated different aspects of cell migration. For instance, tumor growth is the direct result of cell proliferation and cell migration. It has been found that certain integrins facilitate endothelial cell migration and survival during the process of angiogenesis and lymphangiogenesis (Avraamides et al., 2008). Cell migration is regulated by polarity proteins. There are oncogenic signals that can re-localize polarity proteins which lead to tumor invasion and metastasis (Etienne-Manneville, 2008). In 2D modeling cell migration, research involved in using different guiding systems and various chemical molecules have been done to reveal the comprehension of environment cues affecting cell migration.

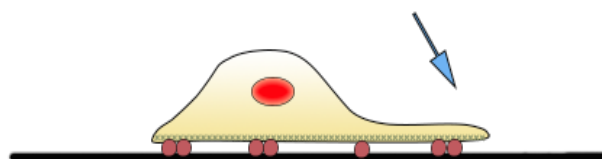
**1. Random moving**



**2. Determine leading and rear sides and form a protrusion**



**3. Adhere the leading side to the substrate**



**4. Release the rear side and contraction of cell body**

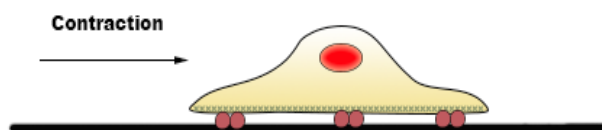


**Figure 1.1 Basic mechanism of cell movement**

1) Random moving cell; 2) Protrusion of the leading edge; 3) Adhesion at the leading edge; 4) Deadhesion at the trailing edge and cell body contract. Adapted from Revathi and Allen 2007.

### ***1.11 Fibroblasts and fibroblast migration***

Fibroblasts, an important cell type in the process of wound healing, synthesize the extracellular matrix (ECM). It is one of the most common cell types of connective tissue in animals. When tissue injury happens, fibroblasts proliferate and migrate towards the wound area, where they produce huge amounts of collagenous matrix. It helps to isolate and repair the injured tissue (Alberts et al., 2002).

During the process of wound healing, there are four stages: homeostasis, inflammation, proliferation, and tissue remodeling or resolution (Guo and DiPietro, 2010). The whole process includes the presence of fibroblasts, angiogenesis, macrophages, and lymphocytes. One possible method to improve the efficiency of wound healing is to control the cells involved in this whole process (Rodriguez-Menocal et al., 2012). Studies have been performed using fibroblasts to investigate diabetic wound healing process (Amos et al., 2010) and to study the interaction of Src and Alpha-V integrin to modulate lung fibrosis (Lu et al., 2017). Some studies utilize human tendon fibroblasts to explore methods that enhance the healing of tendon (Jamil et al., 2017). Another research uses human corneal fibroblasts to investigate the regenerative nature of corneal repair (Gallego-Muñoz et al., 2017). Also, there is a study focusing on chemokine receptors on oral fibroblasts to explore if these receptors have an impact on fibroblast proliferation, migration and the release of wound healing mediators (Buskermolen et al., 2017).

In addition, fibroblasts are a key determinant in the cancer. Fibroblasts in tumors are often referred to as cancer-associated fibroblasts (CAFs). Fibroblast can produce different growth factors, such as fibroblast growth factors (FGFs), which are involved in angiogenesis and various endocrine signaling pathways. These growth factors, as well as chemokines and ECM accelerate angiogenesis, are key factors in tumor progression. Therefore, fibroblasts play a prominent role in the tumor growth and metastasis (Kalluri and Zeisberg, 2006). To better understand and further identify potential targets for tumor treatment, it is important to study the factors influencing fibroblast migration.

### ***1.2 Function of Top2b***

Topoisomerases are enzymes that are involved in positive supercoiling or negative supercoiling of DNA. They are classified into two types: Type I topoisomerase and Type II topoisomerase. Type I topoisomerase cuts one strand of a DNA double helix and releases the supercoiled DNA. Then the cut strand is reannealed. Type II topoisomerase cuts both strands of one DNA double helix, and then it passes an unbroken double-strand DNA through the cut one, thus releasing the supercoiled DNA. Then it reanneals the cut strands (Figure 1.2.1).

Type II topoisomerase can be further classified into two subtypes: Topoisomerase II alpha (Top2a) and topoisomerase II beta (Top2b). They are located on human chromosome 17 and chromosome 3 respectively (Tan KB et al., 1992). It has been found that Top2a is predominately expressed in

proliferating cells, while Top2b is expressed in differentiated cells (Tsutsui et al., 1993; Lyu and Wang, 2003; Zhang et al., 2012). Studies have shown that Top2a is critical for cell proliferation and it functions during chromosome condensation and segregation in proliferating cells (Grue et al., 1998 and Linka et al., 2007). Top2b is only highly expressed in postmitotic cells and it mainly functions during cell transcription (Ju et al., 2006). It has been found that lack of Top2b may have an impact on expression of a subset of genes, particularly reelin (RELN). This results in cortical lamination structure that similar to mutants of the reelin-signaling pathway. However, except for a reduction in RELN expression, much more research needs to be done to reveal other changes (Lyu and Wang 2003). Top2b can release DNA supercoiling by catalyzing the two strands of duplex DNA breaking and rejoining. Recent studies have shown that Top2a can be a primary target of anthracycline's anticancer activity, while Top2b might be related with the development of anthracycline-induced cardiotoxicity (Alvaro et al., 2016).

Knocking out type II topoisomerase has been a useful method to investigate the function of Top2a and Top2b. Data show that Top2b may substitute for Top2a's function during chromosome condensation when Top2a is knocked out, but not chromosome segregation. In Top2b deficiency mice, neural developmental defects are observed such as defective innervation of motor neurons in the diaphragm muscle (Yang et al., 2000), abnormal migration of cerebral cortical neurons, and aberrant lamination of the cerebral cortex (Yang et al., 2000; Lyu and Wang 2003). Research has shown that in embryonic stem



cell-derived neurons, absence of Top2b results in cell death (Tiwari et al., 2012). Top2b knockout retina shows defective laminar structure and neurite outgrowth. It also reduces retinal thickness and leads to apoptotic cell death increase at later developmental stages (Li et al., 2014). Top2b is found to be critical in the repair of double stranded DNA breaks in primary neurons in Ku70 and PARP-1 dependent pathways (Mandraj et al., 2011). In the repair of DNA damage, Top2b plays an important role in melphalan-induced crosslinks in K562 cells (Emmons et al., 2006).

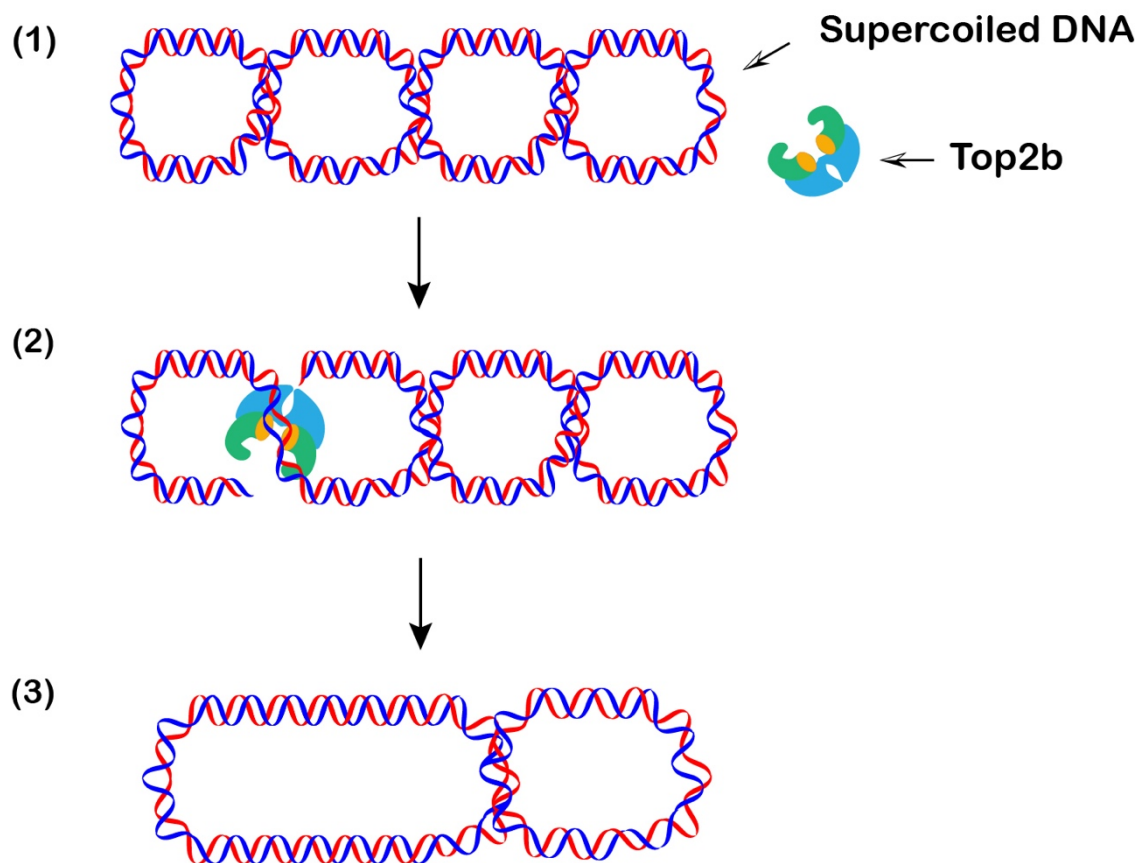


**Figure 1.2.1 Function of Top2b**

1) Shows a supercoiled double-strand DNA and Top2b. 2) Top2b cuts two strands of DNA and passes an unbroken DNA through the cut one. 3) The supercoiled DNA release tension. Adapted from Liam et al., 2014.

### **1.21 Top2b inhibitor ICRF-193**

Catalytic inhibitors have been found to have significant inhibition effect on type II topoisomerase, such as ICRF-193 (Tanabe et al., 1991), merbarone (Drake et al., 1989), aclarubicin (Jensen et al., 1990), forstriein (Boritzki et al., 1988), staurosporine (Lassota et al., 1996) and mitindomide (Hasinoff et al., 1997). They use different mechanisms to inhibit function of topoisomerase. ICRF-193, 4,4-(2,3-butanediyl)-bis(2,6-piperazinedione), is a type II topoisomerase inhibitor, which is known to induce Top2b depletion with the presence of proteasome (Xiao et al., 2002). It is more potent against Top2b than Top2a. The inhibitory mechanism of ICRF-193 on type II topoisomerase is thought to be based on a protein clamp model of eukaryotic DNA topoisomerase II. In this model, a homodimeric enzyme is modulated by ATP. When ATP binds to the protein, two jaws of the clamp close. After the bound ATP is hydrolyzed, the two jaws reopen (Roca, 1994). Research has shown that the inhibitory effect of ICRF-193 on type II topoisomerase is modulated with the presence of ATP. ICRF-193 inhibits ATPase activity of type II topoisomerase, that is ICRF-193 binds with Top2b-ATP complex, which result in a closed clamp position of Top2b (Roca, 1994). This stops the reannealing of DSB and results in proteasomal decomposition of Top2b (Figure 1.2.2), which further leads to abnormal chromosomal condensation and decondensation, as well as cellular apoptosis (Yanagida et al., 1987, Hasinoff et al., 2001). While the biological detail for proteasome-mediated Top2b degradation is still unclear, studies have shown that

small ubiquitin-like modifier (SUMO) pathway is essential in this process (Isik et al., 2003). As a Top2b inhibitor, ICRF-193 has been used in various research to suppress the function of Top2b. By using ICRF-193 to inhibit Top2b, HIV-1 replication is damaged and HIV life cycle is affected, whereas overexpression of Top2b results in increasing HIV-1 replication (Chekuri et al., 2016). A study using ICRF-193 to inhibit Top2b in ventral mesencephalic (VM) neurons shows that these cells have short neurites and growth cones collapsing, which is similar to Top2b siRNA treated VM neurons (Heng et al., 2012). ICRF-193-treated cells show no differences in base excision repair (BER) activity, which suggests that type II topoisomerase itself may not participate in BER activity (Gupta et al., 2002). Also, using ICRF-193 to inhibit Top2b activity in myeloid leukemia cell lines shows an increase in ATRA-induced differentiation and cytotoxicity (Chikamori et al., 2006). In short, ICRF-193 has been a well-established catalytic inhibitors of type II topoisomerase.

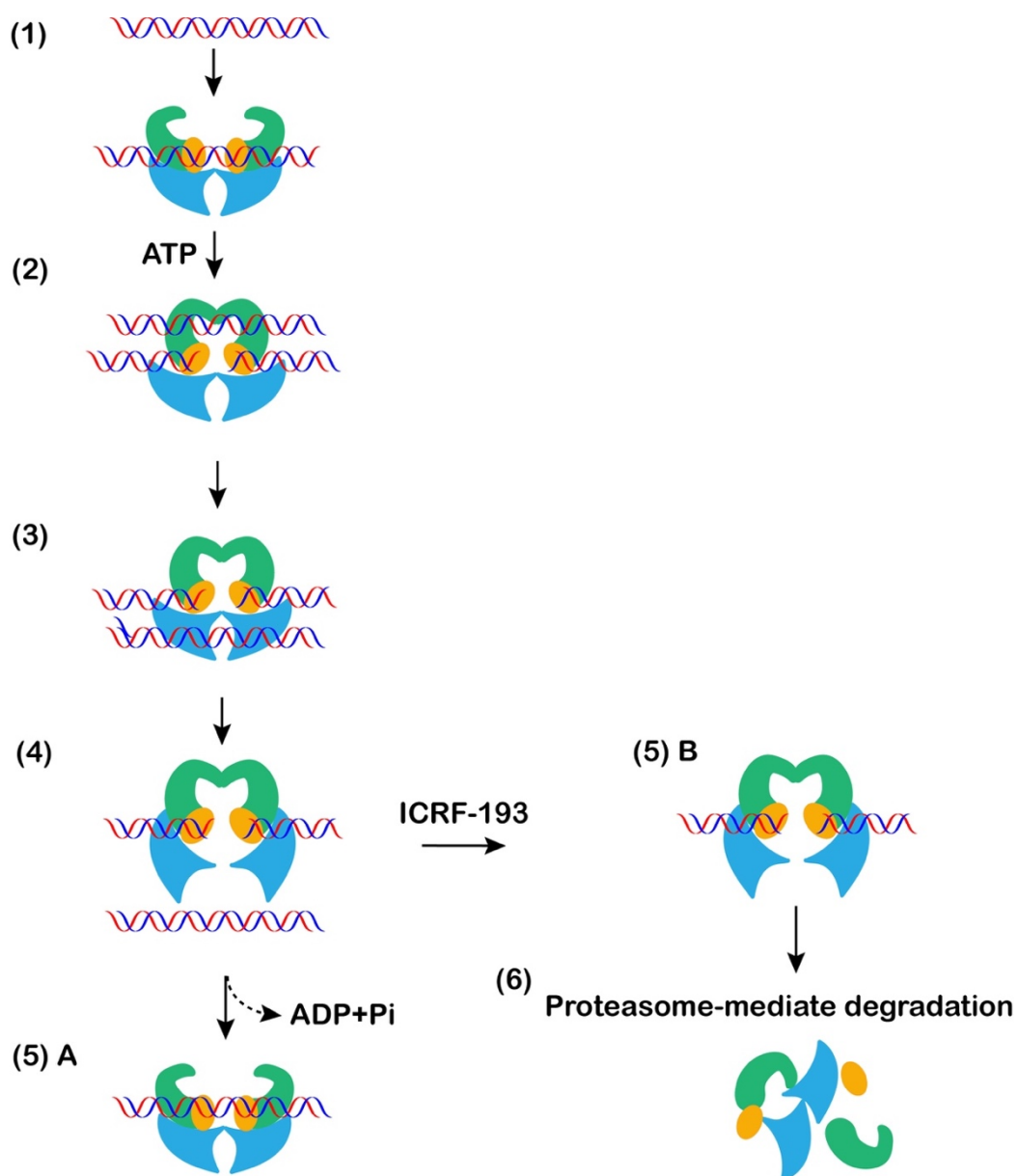


**Figure 1.2.2 Inhibition effect of ICRF-193 on Top2b**

In the protein clamp model, 1) the two subunits of Top2b are open at first. 2) With the presence of ATP, the two clamps close and DNA double strands are cut. 3,4) A uncut double-strand DNA is passed through the cut one. 5A) As ATP hydrolyzes, the cut DNA is rejoined. 5B) ICRF-193 is added and it inhibits ATP hydrolysis, therefore the double strand break cannot be reannealed. 6) This leads to proteasome-mediate degradation of Top2b and further it may cause cellular apoptosis. Adapted from Lyu et al. 2007 and Vejpongsa and Yeh 2014.

### ***1.3 Microfluidic device***

Microfluidics has origins in early 1990's and has been growing rapidly. In recent years, a wide range of studies has been involving microfluidic devices into biomedical research, including drug delivery and tissue engineering. Compared with traditional devices, the micro-sized structures in microfluidic devices allow research to be performed in a more accurate way on a smaller scale, thus improving the precision of experiments. Since microfluidic devices only need a small volume of liquid, they are able to detect changes or results from low volume samples. So far, various kinds of microfluidic devices have been designed to meet different requirements of studies. Many of them are well-established and already commercialized to the public, such as four-chamber devices. These devices have been widely used in biomedical research. For example, the four-chamber neuron device has been used to study axonal outgrowth under different oxygen levels (Qian et al., 2016), the role of Dp427 in nerve growth factor (NGF) dependent axonal growth (Lombardi et al., 2017), the role of miR-145 in capillary tube generation and axonal outgrowth (Cui et al., 2016). Still, more complex microfluidic devices are under development and on their way to the market. A circular compartmentalized co-culture microfluidic device has been presented to be used in the study of central nervous system (CNS) axon myelination research (Park et al., 2009). A paralleled-chamber device has been proposed to study secondary spreading toxicity and the role of GluN2B in this process (Samson et al., 2016). Therefore, the idea of using

microfluidic devices to conduct more precise studies is becoming the leading trend in biomedical field.

#### ***1.4 Rationale***

Top2b has been known to play an important role in neural development. Lack of Top2b may result in premature cell death of embryonic stem cell (ESC)-derived neurons (Tiwari et al., 2012), as well as abnormal retinal development, such as delayed neural differentiation and retina cell number decrease (Li et al., 2014). A previous study has found that Top2b affects neurite outgrowth and axon path finding (Nur-E-Kamal et al., 2007; Nevin et al., 2011). Lack of Top2b was found to affect the expression of a subset of genes, such as reelin, which regulates processes of neuronal migration and positioning through controlling cell-cell interactions. However, most research on Top2b function focuses on neural studies leaving Top2b function in cell migration still unclear. Based on this reason, I designed a study focusing on exploring the function of Top2b in cell migration. My hypothesis is that Top2b may facilitate cell migration. Since fibroblasts are a major cell type in wound healing process and it plays an important role in tumor progression and metastasis (Kalluri and Zeisberg, 2006), I use fibroblast as the target to study Top2b function. I hope that this study can further confirm Top2b as a potential target for preventing the development of tumor.

As previously mentioned, ICRF-193 is a well-established inhibitor for Top2b. A lot of research on Top2b function have been done using ICRF-193 to suppress Top2b function. The main aim of this study is to investigate the Top2b function on cell migration, therefore it is reasonable to use ICRF-193 to inhibit Top2b and observe the changes in cell migration.

Currently, there have been several standard models to measure cell migration *in vitro* (Karamichos et al., 2009), such as scratch-wound assay (Cory et al., 2011), gap closure or cell exclusion zone assay, Transwell or modified Boyden chamber assay and microfluidic assays (Pouliot et al., 2000-2013). For scratch-wound assay and gap closure or cell exclusion zone assay, cells are cultured in the regular cell culture plates or flasks. In the middle of the dish or plate, a cell free area is left where allow cells to migrate to the center. However, the accuracy of these models is questionable since the methods track a group of cells instead of single cell. For Transwell or modified Boyden chamber assay, cells migrate through a membrane with selected pore size. These two assays are suitable for separation of cells or comparison of cell types rather than calculating the cell migration speed. Therefore, a proper cell migration assay for these experiments would be microfluidic devices.



## CHAPTER II MATERIALS AND METHODS

### ***2.1 Design and fabrication***

Firstly, masks were designed and printed at CAD/Art Services, Inc. [Performed in collaboration with Joseph Fantuzzo]. Then a silicon master was produced using standard soft lithography techniques. The first layer was microchannel structures, which was created by spinning SU-8 2002 photoresist (MicroChem) onto a silicon wafer to form a 3  $\mu\text{m}$  layer. This layer was exposed to UV light and developed in SU-8 developer (MicroChem). The two ends of microchannels (10  $\mu\text{m}$  wide, 200  $\mu\text{m}$  long) connected with two chambers which were the obtained through a second layer of resist. Dual-layer of SU-8 2075 and 2025 (MicroChem) were spun onto the wafer to form a 320  $\mu\text{m}$  layer. This second layer was aligned, exposed to UV light and developed. Since the major material of microfluidic devices were polydimethylsiloxane (PDMS), silicon wafer need to be silanized by vapor deposition of Trichloro (1H, 1H, 2H, 2H-perfluorooctyl) silane (Aldrich) for 1 hour to make wafer hydrophobic. Then PDMS with curing agent (ratio 10:1, Sylgard, Dow Corning) was poured onto silicon wafer. After degassing at room temperature for at least 2 hours, it was cured at 65°C overnight. The PDMS devices were then unmolded. There were two kinds of devices used in the experiment (Figure 2.1). The five-chamber microfluidic devices (Figure 2.1 D, E, F) were used for testing cell seeding method and the two-chamber devices (Figure 2.1 A, B, C) were used for observing cell migration. Holes were punched and devices were cut into desired

size (13mm diameter). Devices were cleaned with acetone first for 1 hour in ultrasonic cleaner (FS60, Fisher Scientific). After they were dried thoroughly, devices were cleaned with isopropyl alcohol (IPA), dried thoroughly and cured at 80°C overnight. Before bonding to glass coverslips, devices were taped to make sure they were free of any dusts or residues. PDMS devices were irreversibly bonded to glass coverslips (48366-067, VWR) using oxygen plasma. All the devices were treated with oxygen plasma to make PDMS surface hydrophilic and were then kept in DI water until they were seeded with cells.

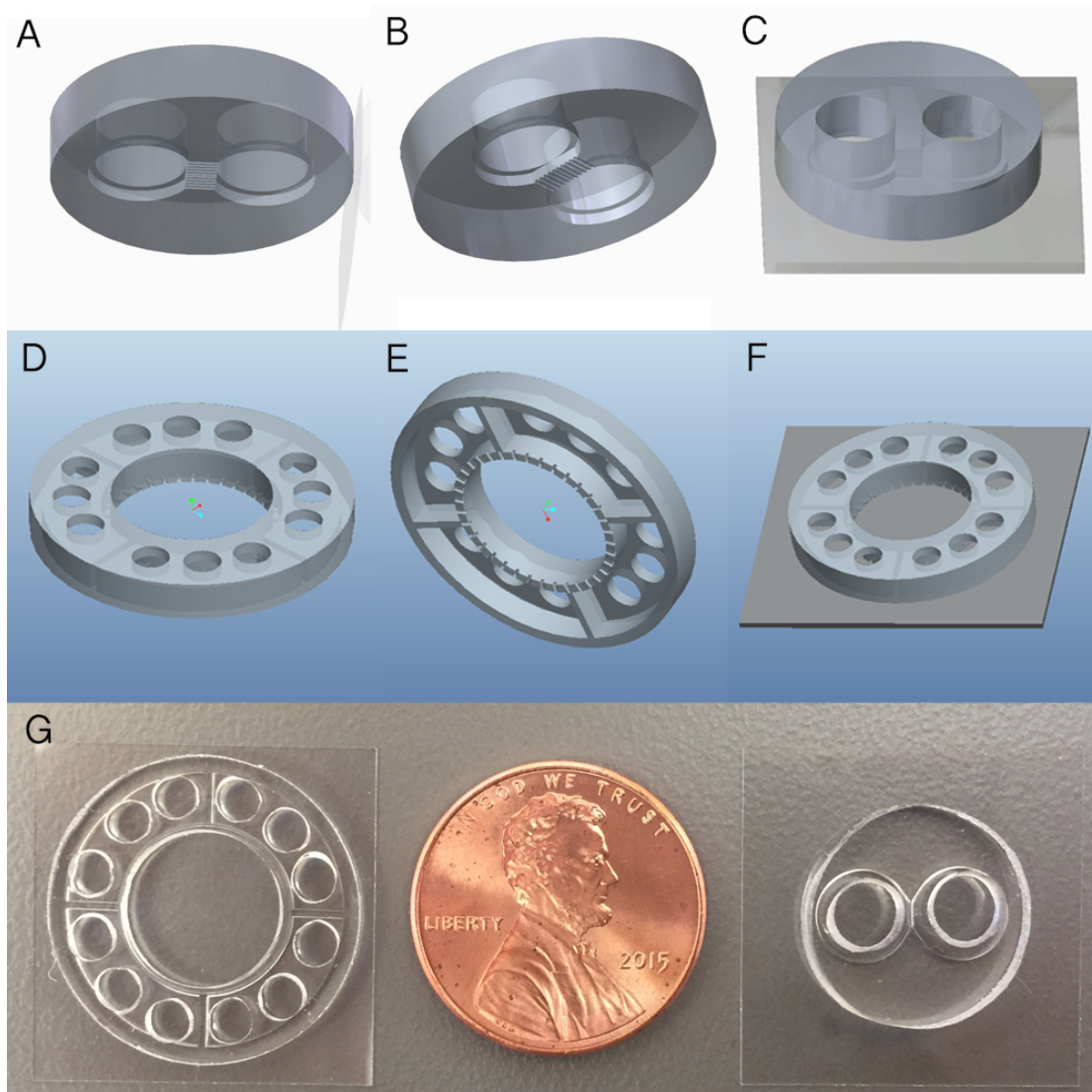


**Figure 2.1 Two kinds of microfluidic device**

A-B) show the design of two-chamber microfluidic device. The diameter of the whole device is 13 mm and the diameter of each chamber is 4.5 mm. The height of PDMS device is 3 mm. Between the two chambers there are 22 microchannels with 10  $\mu\text{m}$  in width and 200  $\mu\text{m}$  in length; D-E) show the five-chamber microfluidic device (20 mm in diameter). Four Chambers are on the side and one big chamber (10 mm in diameter) in the center. Each side chamber, which has three seeding holes (3 mm in diameter), is connected to the center chamber via microchannels. Microchannels have the same dimension as the two-chamber device. C, F) Both devices are irreversibly bonded to glass coverslips via plasma treatment. Coverslips are 22 mm X 22 mm. G) shows the size of both devices when compared with a penny.

## ***2.2 Animals and isolation of mouse primary fibroblasts***

All animal experiments performed were approved by the Institutional Animal Care and Use Committee (IACUC) and the Institutional Biosafety Committee at Rutgers University. All animal work was conducted in accordance with relevant guidelines and regulations of the IACUC.

Primary fibroblasts were prepared from P1 mice of both sexes. First tails were dissected and minced. To disassociate fibroblasts from tissues, tissue was then suspended in 0.25% Trypsin with 2.21mM EDTA and incubated at 37°C for 3 minutes. The cell tissue mixture was filtered by 40  $\mu$ m cell strainer (Fisherbrand). The resultant cell suspension was spun down and the pellet resuspended in cell culture medium, consisting of 89% DMEM (Gibco, Life Technologies), 10% fetal bovine serum (FBS, Gibco, Life Technologies) and 1% penicillin and streptomycin. Cells were then cultured in 6-well plate before they were loaded into devices.

## ***2.3 Device sterilization and cell loading***

Devices were sterilized under UV light for 1 hour with all chambers filled with sterilized phosphate-buffered saline (PBS, Fisher Scientific). After all the preprocessing procedure for devices, they were ready for cell loading. Cells were seeded at density 700 cells/ $\mu$ l for fibroblasts in 45  $\mu$ l of medium. Medium was exchanged every other day for 7 days.

## ***2.4 Treatment with Top2b inhibitor ICRF-193***

For dose-response experiments, cell culture medium with certain concentration of ICRF-193 (0.1  $\mu$ M to 50  $\mu$ M) were added to both culture chamber and migration chamber in microfluidic devices. For control groups, equal concentration of DMSO with cell culture medium were added. Medium supplemented with particular concentration of ICRF-193, were changed every two days.

## ***2.5 Imaging***

Fibroblasts were imaged using inverted motorized microscope (Zeiss Axio Observer Z1) with an AxioCam MRc digital camera (Zeiss, Germany). All images were taken with similar exposure time to ensure comparison. Brightness and contrast were adjusted using AxioVision Rel. 4.8. Number of the cells were counted manually.

## ***2.6 Time-lapse microscopy***

Fibroblast migration was recorded using inverted fluorescent microscope (IX81, Olympus) equipped with a time-lapse system. All images were taken with Hamamatsu EM CCD digital camera, with objective 10x at regular time lapse (5 min) over a 12 hours' period and exported as TIFF files. Images were adjusted using SlideBook 5.0 and Adobe Photoshop CC to ensure each image had similar brightness and contrast.

## ***2.7 Data analysis***

The number of cells were counted manually each day after cell loading to devices for 7 days. Images from time-lapse microscopy were imported to Image J to do further analysis. Tracking analysis was performed by Image J manual measurement. The speed of fibroblast migration was calculated using the distance fibroblasts travel within a certain amount of time. Three to five out of sixteen cells were picked from each video for calculation. For statistical analysis, ANOVA followed with t-tests, as well as Bonferroni correction were used to compare the differences between groups.  $P < 0.05$  is considered statistically significant.

## CHAPTER III RESULTS

### ***3.1 Microfluidic device is an excellent system for cell migration study***

The first aim of experiment was to identify the feasibility of using microfluidic device to culture fibroblasts and observe cell proliferation and migration. The seeding method was firstly tested using five-chamber microfluidic devices. After sterilization, all the devices were loaded with fibroblasts at density 300 cells/ $\mu$ l. Observation began from one day after cell loading and no fibroblasts migration was observed on the first three days. At day4, fibroblasts began to migrate to the center chamber via microchannels and two cells were observed in the center chamber (Figure 3.1.1 A, B). Later in the study higher number of cells were found in the center chamber. This confirms that the device and microchannels were suitable for fibroblasts migration. Next step, the two-chamber devices were prepared for cell seeding. For this device, since the chamber size and volume is different from five-chamber device, a right seeding density needs to be figured out. Since the density of 300 cells/ $\mu$ l results in migration at day4, a density of 1000 cells/ $\mu$ l was applied for the new device in order to observe migration at an earlier stage. However, 1000 cells/ $\mu$ l resulted in some cells death after 2 days of culture which indicated that too many cells in one chamber. Therefore, for the third trial, a density of 700 cells/ $\mu$ l was used for devices. Fibroblast migration was observed at day1. At day 3 many cells were observed in the migration chamber (Figure 3.1.1 C, D, E).

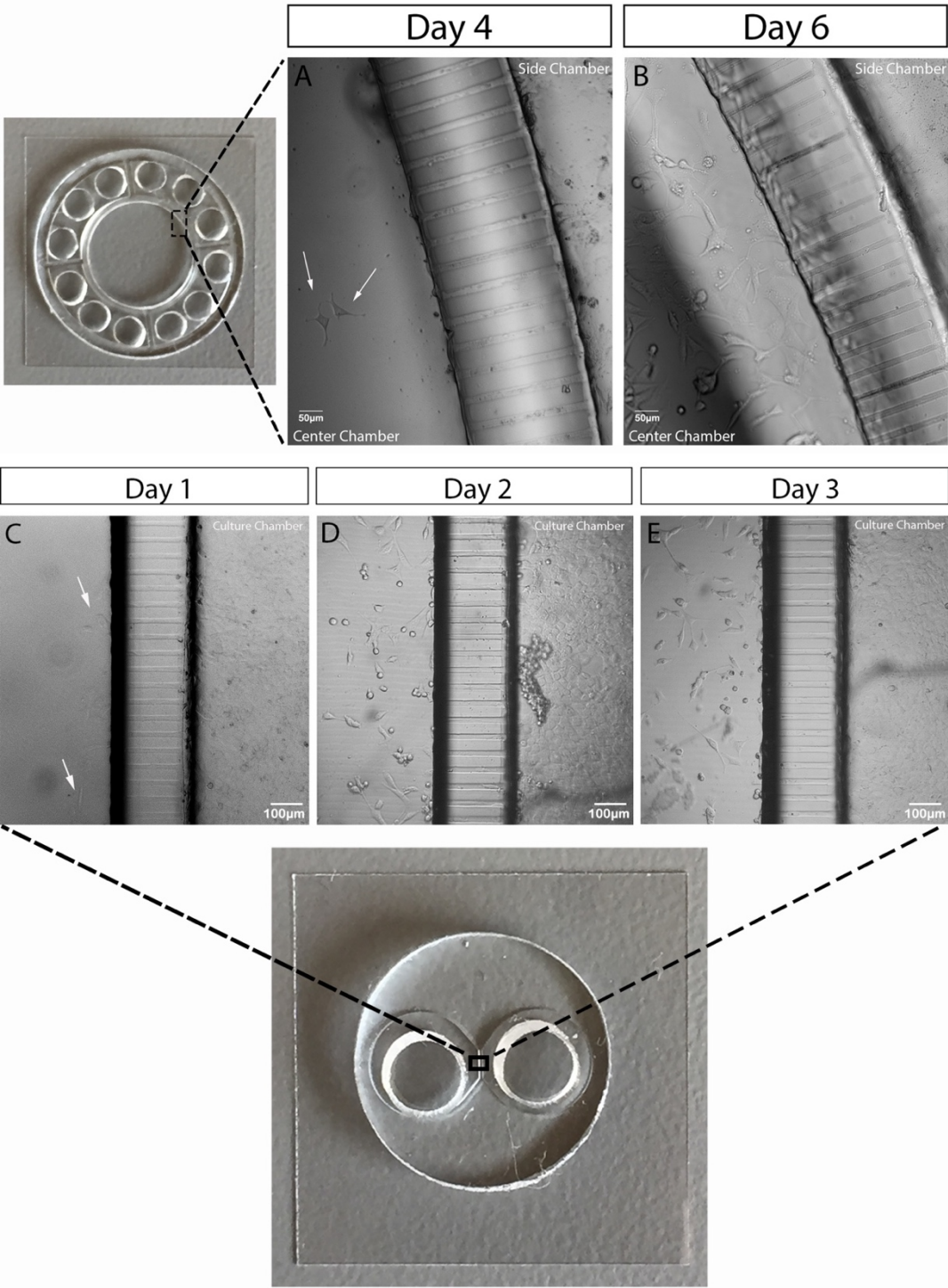




### Figure 3.1.1 Cell culture in microfluidic devices

A-B) show cell culture in five-chamber microfluidic device. A) shows two cells were observed in the center chamber (migration chamber) at day4 (pointed out by arrows). B) shows many cells migration to the center chamber at day6. Images are taken with objective 10x. C-D) show cell culture in two-chamber microfluidic device. C) shows after increasing the seeding density to 700 cells/ $\mu$ l, migration was observed at day1. D-E) at day2 and day3, more cells were observed in the migration chamber.

This experiment was performed in triplicates. At each day the number of cells in the migration chamber was counted manually and recorded (Figure 3.1.2). Results showed that fibroblasts continuously migrated to the other chamber and it confirmed that the microfluidic device is a good model for studying cell migration.

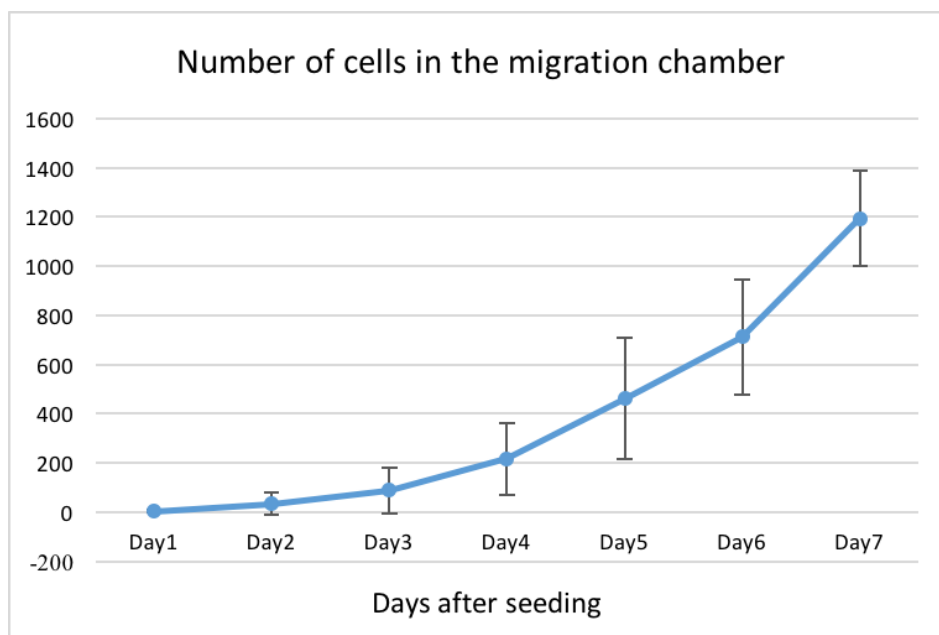


### Figure 3.1.2 Number of cells in the migration chamber

Fibroblast cells were cultured in regular cell culture medium (DMEM) with a seeding density of 700 cell/ $\mu$ l. The number of fibroblast cells that migrated through the channel and reached the other chamber were counted manually at each day from day1 to day7. The number of fibroblast cells in the migration chamber continuously increased.  $n \geq 3$

### 3.2 Fibroblasts migrate into and through microchannel structures

When fibroblasts were cultured in chamber or in tissue culture dish, cells were bipolar or multipolar with elliptic shapes. Once the fibroblast was ready to migrate via microchannel, one of its poles began to explore the entrance of the microchannel. After the pole of the cell recognized the microchannel, the whole cell body began to move to entrance. The exploring pole became the leading side of the cell and cell body squeezed into the microchannel. When fibroblasts were inside channel, cell bodies have a significant change in shape: majority of cells became bipolar with elongated shapes (Figure 3.2.1).

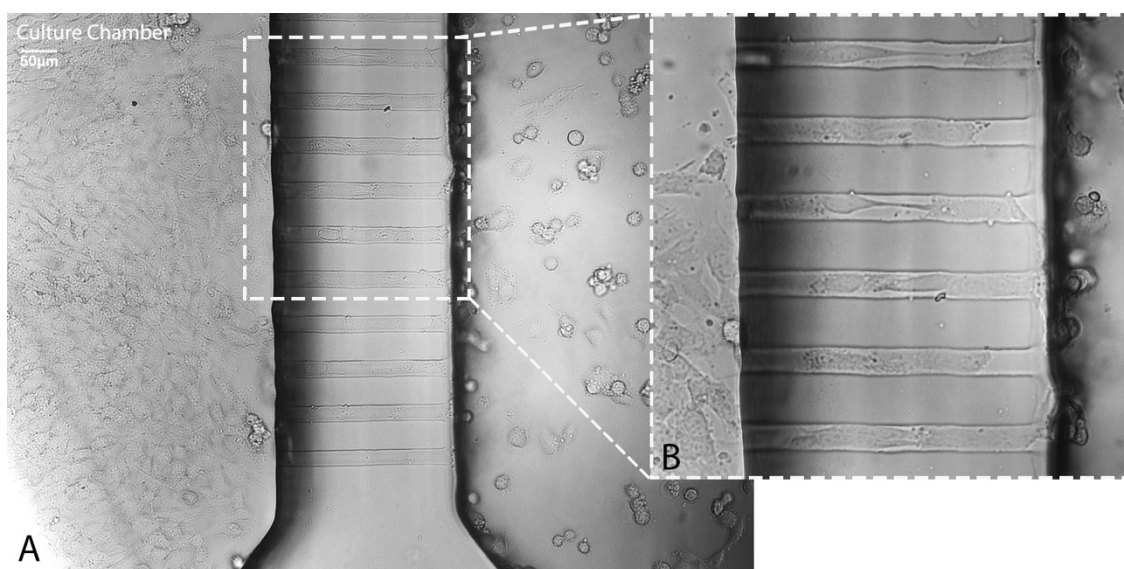


**Figure 3.2.1 Fibroblasts migrate through microchannels**

Panel A shows a representative image of cell culture on two-chamber microfluidic device. Panel B shows the higher magnification of microchannels in boxed area in panel A. Bipolar shaped fibroblasts were observed in the microchannels with the elongated cell bodies. Dimension of microchannels: 10  $\mu\text{m}$  in width and 200  $\mu\text{m}$  in length. Images were taken at day3.

### ***3.3 Top2b inhibition by ICRF-193 suppresses fibroblast migration***

In order to explore the function of Top2b on cell migration, 500  $\mu\text{M}$  ICRF-193 was diluted into different concentrations and then were applied to cell medium. Since the aim of this research is to precisely measure the decrease of fibroblast migration using different concentrations of ICRF-193, a specific range of concentrations needs to be found where the reduction effect is the most. It has been known that inhibition of the ATPase activity by ICRF-193 mostly lies between 0 and 50  $\mu\text{M}$  (Hu et al., 2002). Therefore, three concentrations of ICRF-193 were tested, which are 1  $\mu\text{M}$ , 25  $\mu\text{M}$  and 50  $\mu\text{M}$ . However, cell death was observed at day3 with 25  $\mu\text{M}$  and 50  $\mu\text{M}$  of ICRF-193.

Next, the range of concentration was reduced to 0.1  $\mu\text{M}$ , 1  $\mu\text{M}$  and 10  $\mu\text{M}$ . This time remarkable differences in fibroblast migration among different groups were observed. In the experiment, two control groups were used to compare with experimental groups. Fibroblasts culturing with DMEM (cell medium) was the first control group. Since ICRF-193 was diluted in DMSO, the second control group was fibroblast culturing with DMSO, with a liquid concentration the same as the concentration adding to dilute 0.1  $\mu\text{M}$  ICRF-193. Both treatment groups and control groups were observed continuously for 7 days. At day1, very few or no cell migration was observed in both treatment groups and control groups. At day2, fibroblast migration was observed in two control groups, 0.1  $\mu\text{M}$  ICRF-193, 1  $\mu\text{M}$  ICRF-193 and 10  $\mu\text{M}$  ICRF-193. From day3, significant differences can be found in the number of cells in the migration chamber among different groups (Figure

3.3.1). For the two control groups and 0.1  $\mu$ M ICRF-193 group, cells number increased significantly as the experiment was going on (Figure 3.31 A, B, C). No significant difference was found among these three groups, which indicated that 0.1  $\mu$ M ICRF-193 has little effect on fibroblast migration. For 1  $\mu$ M ICRF-193 group, cell number in the migration chamber also increased, but much slower than the previous groups (Figure 3.3.1 D), whereas for 10  $\mu$ M ICRF-193 group, cells were basically motionless. Only about 10 cells were observed in the migration chamber after 7 days (Figure 3.3.1 D). All the results above suggested that inhibition of Top2b function may result in decreasing fibroblast migration.

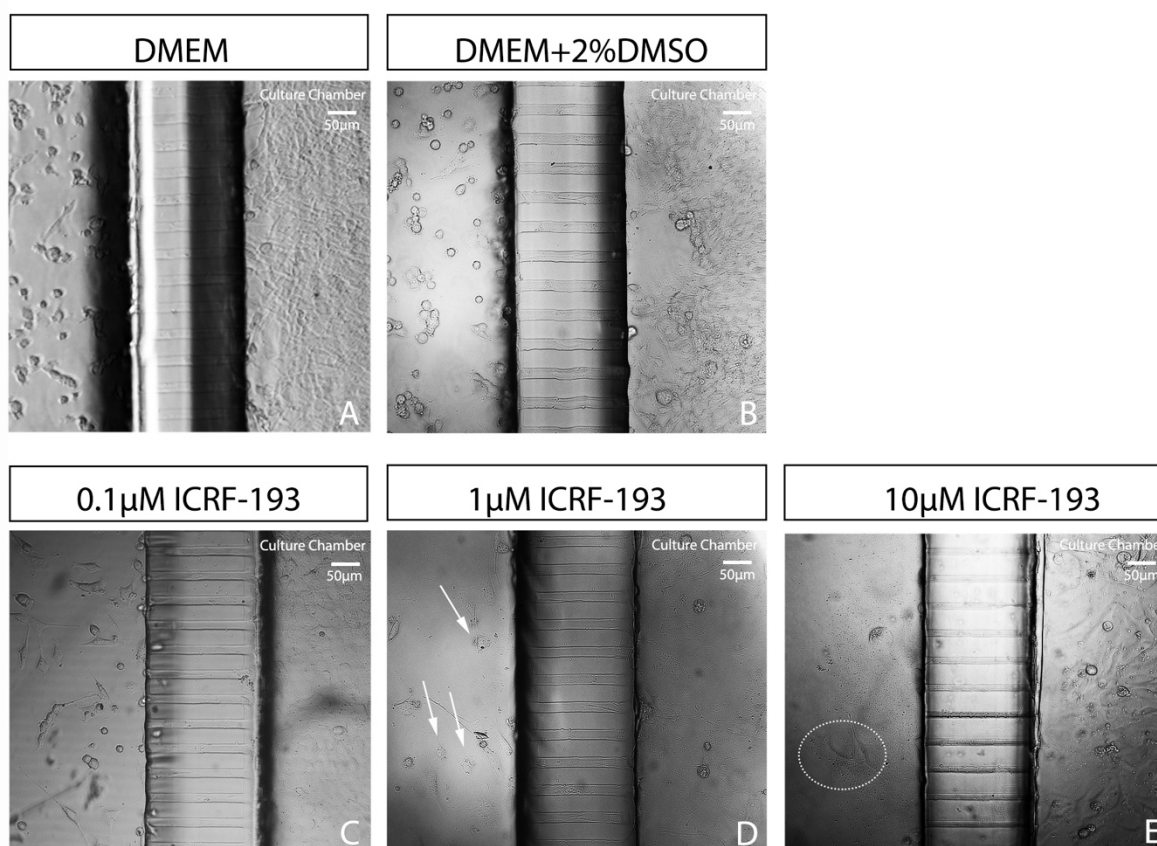


**Figure 3.3.1 Top2b inhibition by ICRF-193 reduces fibroblast cell migration**

Microphotographs show fibroblast cell culture four days after cell seeding in the microfluidic devices. Panels A and B show fibroblast cells cultured with DMEM and DMSO as control groups. Many cells can be observed migrated into the other chamber. Panel C-E shows fibroblast cell culture with 0.1 μM, 1 μM and 10 μM ICRF-193, respectively. Compared with control groups, the number of cells migrated through the microchannels was reduced significantly. Only two migrated cells were observed in the treatment with 10 μM ICRF-193. All images were taken at day3.

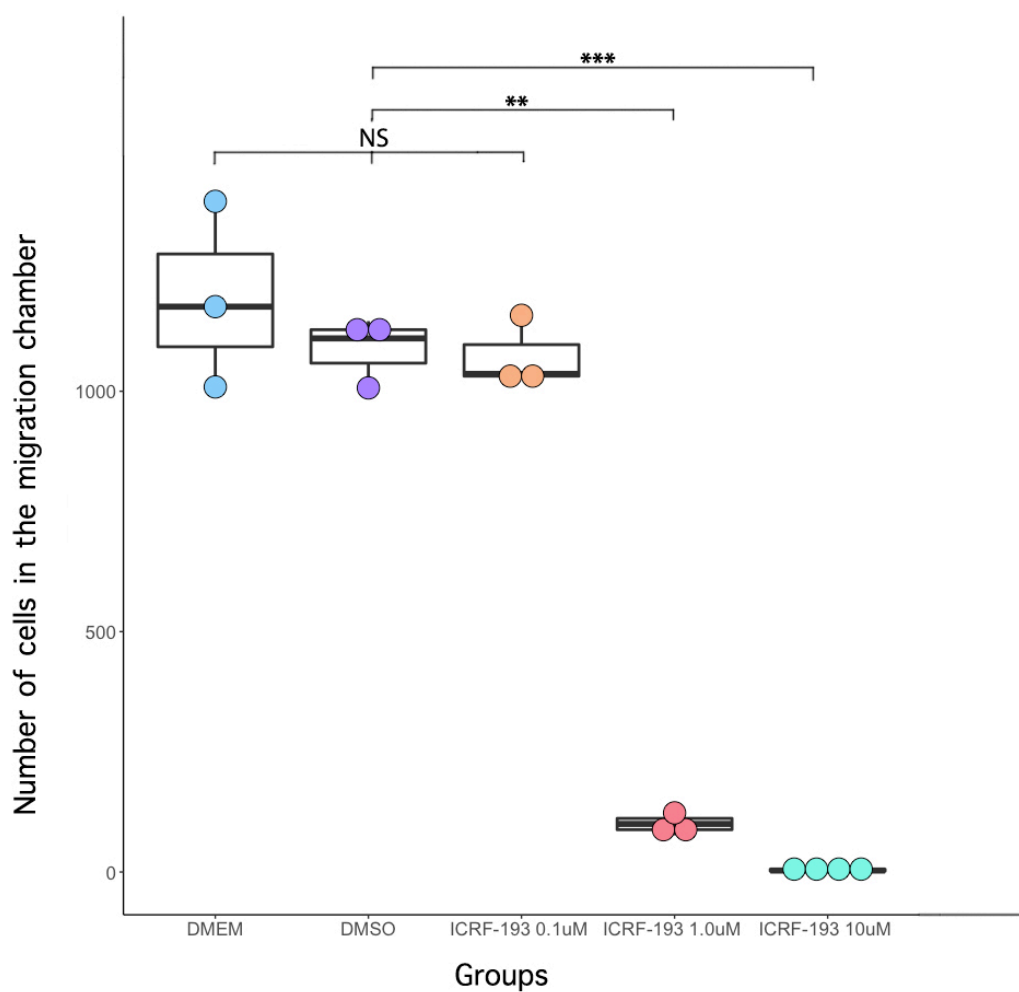


**Figure 3.3.2 Statistical analysis of fibroblast cell migration under Top2b inhibition by ICRF-193**

Number of cells in the migration chamber was counted at day7 for each group. ANOVA analysis was performed followed by Bonferroni correction. \* $p < 0.05$ ; \*\* $p < 0.01$ ; \*\*\* $p < 0.001$ .  $n \geq 3$ .

### ***3.4 Top2b inhibition by ICRF-193 suppresses fibroblast movement***

Since inhibition of Top2b function using ICRF-193 had a negative effect on fibroblast migration, it is reasonable to make the hypothesis that ICRF-193 would also influence the velocity of cell movement. To confirm my hypothesis, I did time-lapse imaging for each device with different concentrations of ICRF-193. At day 1 not many cells were active and after 4 days, some areas of the microfluidic devices were already confluent and that would reduce fibroblast movement. Therefore, to ensure the velocity measured correctly represent cell movement, all the videos were recorded overnight using seeded devices from the second day to fourth day. Speed was calculated by tracking the front edge of cells. Compared with the control groups, treatment groups with different concentrations of ICRF-193 shows reduced velocity in fibroblast migration (Figure 3.4.1). As concentration increasing, the speed of fibroblast migration decreased. Time-lapse videos show fibroblasts cultured with culture medium have a migration speed of  $0.77 \pm 0.14 \mu\text{m}/\text{min}$ ; when fibroblasts cultured with culture medium supplemented with DMSO, fibroblasts have a migration speed of  $0.85 \pm 0.53 \mu\text{m}/\text{min}$ ; fibroblasts cultured with  $0.1 \mu\text{M}$  ICRF-193 in culture medium have a migration speed of  $0.64 \pm 0.30 \mu\text{m}/\text{min}$ ; fibroblasts cultured with  $1 \mu\text{M}$  ICRF-193 have a migration speed of  $0.47 \pm 0.21 \mu\text{m}/\text{min}$  and fibroblasts cultured with  $10 \mu\text{M}$  ICRF-193 have a migration speed of  $0.14 \pm 0.17 \mu\text{m}/\text{min}$ ; Statistical analysis shows that there are significant differences between control groups and treatment group with  $10 \mu\text{M}$  ICRF-193 (Figure 3.4.2).

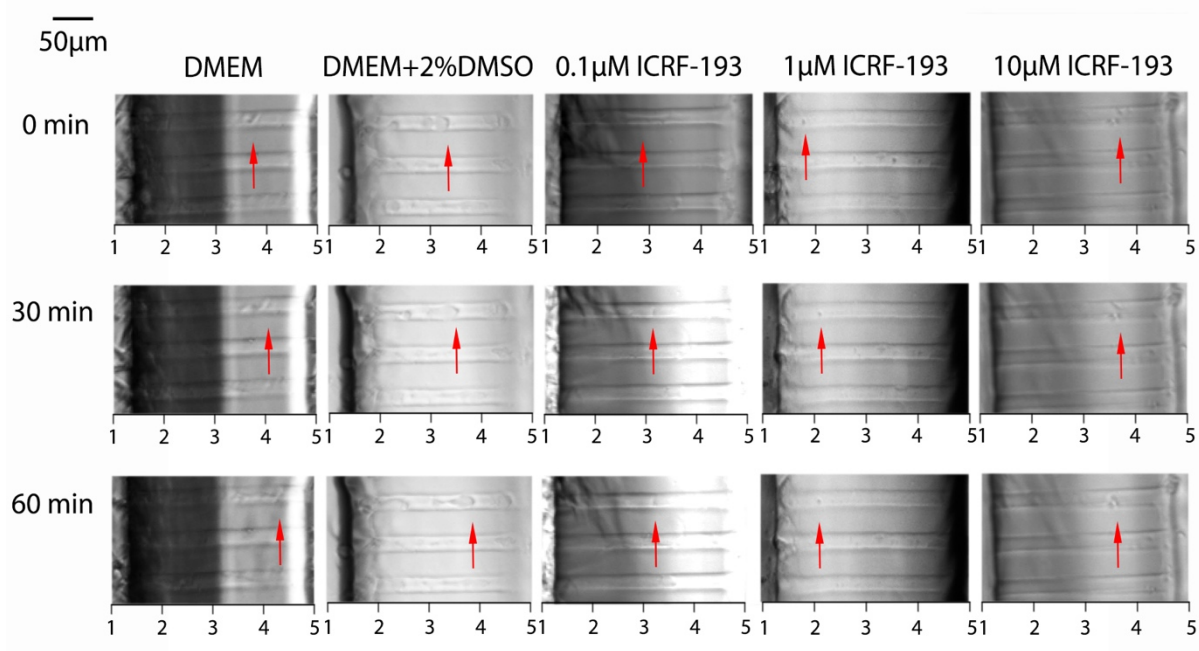


**Figure 3.4.1 Top2b inhibition by ICRF-193 decreases the speed of fibroblast migration**

Microphotographs of cultured fibroblasts in microchannels 0 min, 30 min, and 60 min after ICRF-193 treatment. As the concentration of ICRF-193 increases, the speed fibroblast cell migration decreases.



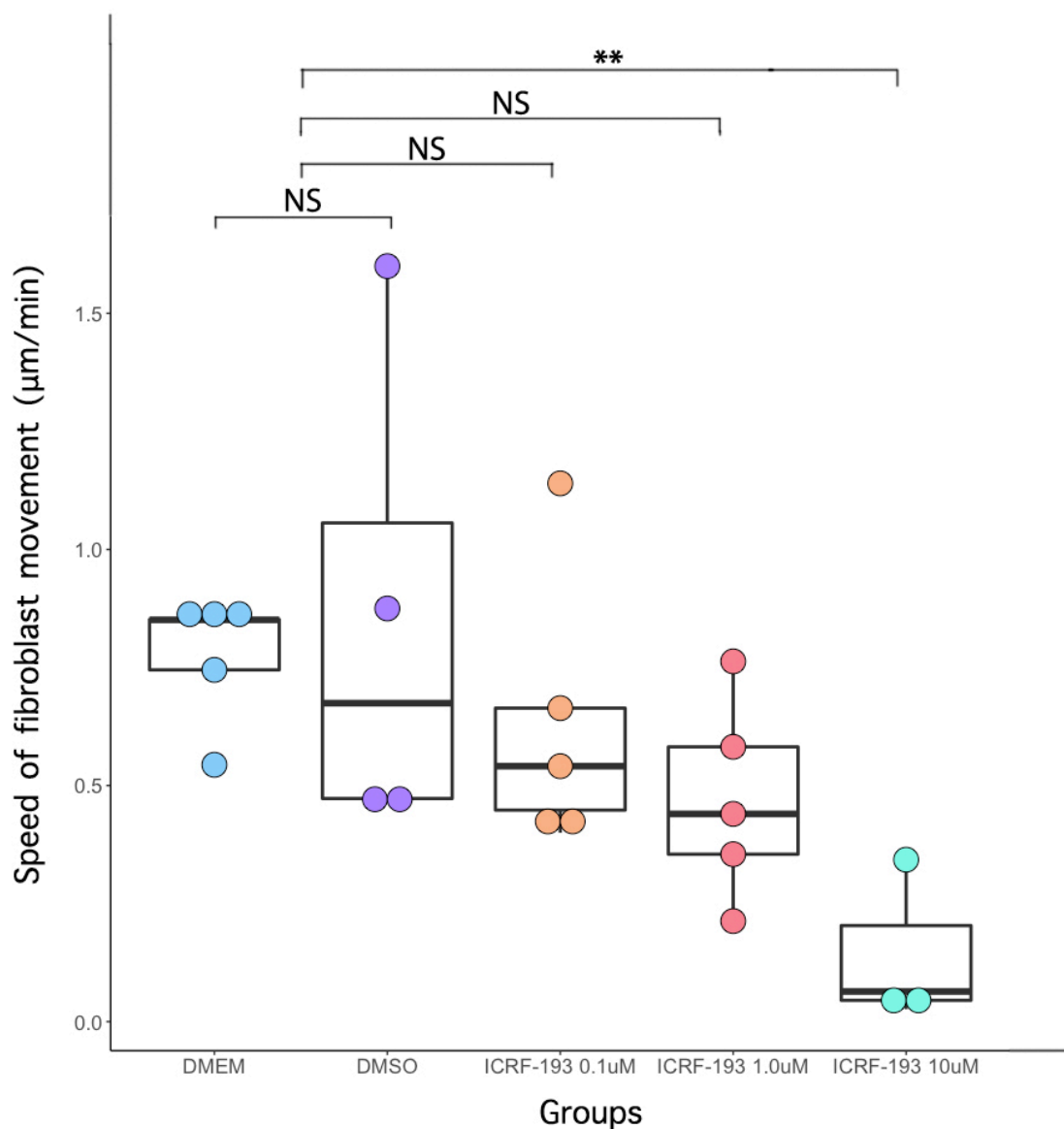


**Figure 3.4.2 Statistical analysis of the speed of fibroblast cell migration under Top2b inhibition by ICRF-193**

Compared with the two control groups, the speed of fibroblasts migration was significantly reduced with 10  $\mu\text{M}$  ICRF-193. Statistical difference is obtained by ANOVA analysis followed with Bonferroni correction. \* $p < 0.05$ ; \*\* $p < 0.01$ ; \*\*\* $p < 0.001$ .  $n \geq 3$ .

## CHAPTER IV DISCUSSION

In this study, I used microfluidic devices as a tool to investigate the inhibition effect of Top2b by ICRF-193 on fibroblast migration and precisely calculate the speed of fibroblast migration. By treating cells with various concentrations of ICRF-193 (e.g., 0.1  $\mu$ M, 1  $\mu$ M, and 10  $\mu$ M), we determined that inhibiting Top2b function reduces fibroblast movement and the number of cells migrated through the microchannels.

The innovation of this study is combination of microfluidic device with the study of Top2b function on cell migration. Cell culture on microfluidic device for precise research has been a trend in biomedical field. This results show that fibroblasts spontaneously adjust cell bodies as they entering microchannels and moving along the channel structure. Similar results from previous studies have been found using different cell types, such as microglia spontaneously adjust to the structures (Amadio et al., 2013). Since cell culture on this microfluidic device is very successful, this model is suitable for further cell analysis. Especially as the width of the channel only allows single cell to enter (Figure 3.2.1), single cell analysis can be done on this device such as: single cell imaging. This device is also capable of performing chemical gradient by adding chemicals to one chamber and the solvent will automatically diffuse along microchannels. Also, capillary electrophoresis can be done on this device, due to small fluid volumes consumption. Even though in this study I show a very basic usage of this device, it is actually a very promising device for various kinds of research.

In this study, fibroblast were treated with different concentrations of ICRF-193. Results showed that dose of 25  $\mu$ M and 50  $\mu$ M of ICRF-193 cause cell death. This is consistent with results from previous study that ICRF-193 is able to induce apoptotic cell death by interfering DSB rejoining (Hasinoff et al., 2001). By using low dose of ICRF-193 significant cell death was not observed. However, if high dose of ICRF-193 is used in research, it would be hard to tell if the change in cells is the result of Top2b or cytotoxicity of ICRF-193. Still, more research need to be done to reveal the effect of ICRF-193 on cell death.

Also, previous studies have been done on exploring Top2b function in neural development. Top2b is found to be essential for neurite outgrowth and axon path finding (Nur-E-Kamal et al., 2007; Nevin et al., 2011). When Top2b was inhibited, shorten VM neurites and collapsed growth cones were observed in primary culture (Heng et al., 2012). These results suggested that Top2b have a role in regulating cell exploring the surroundings. However, no research has been done to precisely measure the number of cell migration using Top2b inhibitor. By increasing the dose of ICRF-193, I showed significant differences in reduction of fibroblast migrating to the migration chamber (Figure 3.3.1), which was almost 10 fold of number decreasing between each two doses. This result strongly indicated the presence of Top2b can facilitate fibroblast migration. As it is known that fibroblasts are highly involved in the progression of tumor growth and metastasis, this character of Top2b suggested that it can be a potential target for anti-cancer drugs. Wounds, especially chronic wounds which is still the major

cause of illness for patients (Rodriguez-Menocal et al., 2012). Since fibroblast is an essential cell type during the wound healing process, fibroblast migration needs to be promoted in order to have a better prognosis for patients. Based on my study, it may be helpful to upregulate Top2b to facilitate wound healing.

Another innovation of my study is the precise measurement of speed of fibroblast migration under inhibitory effect of ICRF-193. Previous study has been done using microfluidic devices to calculate the speed of neurite outgrowth under different oxygen level (Qian et al., 2016). However, few research was focusing on Top2b function on fibroblast migration. My results were the first to measure the precise speed of fibroblast migration with inhibition of Top2b by ICRF-193. It showed that as the concentration of ICRF-193 increased, the speed of cell migration decreased significantly from  $0.77 \pm 0.14 \mu\text{m}/\text{min}$  (control group) to  $0.64 \pm 0.30 \mu\text{m}/\text{min}$  ( $0.1 \mu\text{M}$  ICRF-193),  $0.47 \pm 0.21 \mu\text{m}/\text{min}$  ( $1 \mu\text{M}$  ICRF-193) and  $0.14 \pm 0.17 \mu\text{m}/\text{min}$  ( $10 \mu\text{M}$  ICRF-193). This result is consistent with previous study that fibroblasts have an average moving speed of less than  $1 \mu\text{m}/\text{min}$  (Trepats et al., 2012). It also strongly suggested that by inhibiting Top2b function in fibroblast, the speed of cell migration can be controlled and it sheds light on precise research of cell migration. By knowing the accurate speed of fibroblast migration under inhibitory effect of ICRF-193, next step we may establish a fibroblast migration model based on this inhibitory effect. In addition, using this model we can accurately control the speed of the fibroblast migration via applying a certain concentration of ICRF-193, which would be a useful tool to

further analyze the relation between Top2b and cell migration. For instance, we can figure out which gene is turned on or off by targeting Top2b with ICRF-193 during fibroblast migration. This may help us to obtain a better idea on the regulatory function of Top2b on cell migration.

However, there are still some issues needs to be addressed in this research. For example, the number of cells in the migration chamber is the total number of fibroblasts from migration and cell proliferation. This is the reason that the number of cells in the migration chamber (Figure 3.1.2) has a trend of curved line rather than a straight line. To obtain a more accurate result, proliferated cells need to be separated from migrated cells. The expected result of number of pure migrated cells is a straight line. Therefore, for future research Ki-67 protein, a cellular marker for proliferation, will be labeled in cells and only migrated fibroblasts will be counted in the migration chamber. Moreover, to strengthen the result that reduction in number of cells in the migration chamber is due to Top2b regulation rather than cellular apoptosis, stem cell factor (SCF) will be used in the future research. SCF has been found to promote cell survival and proliferation in lots of cell types, such as vascular smooth muscle, germ cells and hematopoietic stem and progenitor cells (Wang et al., 2007; Yan et al., 2000; Hassan and Zander 1996). Therefore, next step for each concentration of ICRF-193, there will be a corresponding SCF control group to confirm that reduction in number of cells in migration chamber is not due to apoptosis.

## REFERENCES

- Alberts, B. Johnson, A. Lewis, J, et al. (2002) *Molecular Biology of the Cell*, 4th edition. New York: Garland Science; ISBN-10: 0-8153-3218-1 ISBN-10: 0-8153-4072-9.
- Alvaro Mordente, Elisabetta Meucci, Giuseppe Ettore Martorana, Daniela Tavian and Andrea Silvestrini. (2016). Topoisomerases and Anthracyclines: Recent Advances and Perspectives in Anticancer Therapy and Prevention of Cardiotoxicity, *Current Medicinal Chemistry*, volume 23, issue , pages 1-20, issn 0929-8673/1875-533X, doi 10.2174/0929867323666161214120355
- Amadio, S., De Ninno, A., Montilli, C., Businaro, L., Gerardino, A., & Volont, C. (2013). Plasticity of primary microglia on micropatterned geometries and spontaneous long-distance migration in microfluidic channels. *BMC Neuroscience*, 14(1), 1–1. <http://doi.org/10.1186/1471-2202-14-121>
- Amos, PJ. Kapur, SK. Stapor, PC. Shang, H. Bekiranov, S. Khurgel, M. Rodeheaver, GT. Peirce, SM. Katz, AJ. (2010). Human Adipose-Derived Stromal Cells Accelerate Diabetic Wound Healing: Impact of Cell Formulation and Delivery. *Tissue Engineering*, 1–12. <http://doi.org/10.1089/ten.tea.2009.0616>
- Ananthakrishnan, R, Ehrlicher, A. (2007). The Forces Behind Cell Movement. *The Forces Behind Cell Movement*, 1–15.
- Avraamides, C. J., Garmy-Susini, B., & Varner, J. A. (2008). Integrins in angiogenesis and lymphangiogenesis. *Nature Reviews Cancer*, 8(8), 604–617. <http://doi.org/10.1038/nrc2353>
- Boritzki, T. J., Wolfard, T. S., Besserer, J. A., Jackson, R. C., and Fry, D. W. (1988). Inhibition of type II topoisomerase by fostriecin. *Biochem. Pharmacol.* 37, 4063–4068
- Buskermolen, J. K., Roffel, S., & Gibbs, S. (2017). Stimulation of Oral Fibroblast Chemokine Receptors Identifies CCR3 and CCR4 as Potential Wound Healing Targets. *Journal of Cellular Physiology*, 1–24. <http://doi.org/10.1002/jcp.25946>
- Chekuri, A., Bhaskar, C., Bollimpelli, V. S., & Kondapi, A. K. (2016). Topoisomerase II $\beta$  in HIV-1 transactivation. *Archives of Biochemistry and Biophysics*, 593(C), 90–97. <http://doi.org/10.1016/j.abb.2016.02.009>
- Chikamori, K., Hill, J. E., Grabowski, D. R., Zarkhin, E., Grozav, A. G., Vaziri, S. A. J., et al. (2006). Downregulation of topoisomerase II $\beta$  in myeloid leukemia cell lines leads to activation of apoptosis following all-trans retinoic acid-induced differentiation/growth arrest. *Leukemia*, 20(10), 1809–1818. <http://doi.org/10.1038/sj.leu.2404351>

Cory G. Scratch-wound assay. *Methods Mol Biol.* 2011;769:25–30. [http://dx.doi.org/10.1007/978-1-61779-207-6\\_2](http://dx.doi.org/10.1007/978-1-61779-207-6_2).

Cui, C., Ye, X., Chopp, M., Venkat, P., Zacharek, A., Yan, T., et al. (2016). miR-145 Regulates Diabetes-Bone Marrow Stromal Cell-Induced Neurorestorative Effects in Diabetes Stroke Rats. *STEM CELLS Translational Medicine*, 5(12), 1656–1667. <http://doi.org/10.5966/sctm.2015-0349>

Drake, F. H., Hofmann, G. A., Mong, S. M., Bartus, J. O., Hertzberg, R. P., Johnson, R. K., Mattern, M. R., and Mirabelli, C. K. (1989). In vitro and intracellular inhibition of topoisomerase II by the antitumor agent merbarone. *Cancer Res.* 49, 2578–2583

Emmons, M., Boulware, D., Sullivan, D. M., & Hazlehurst, L. A. (2006). Topoisomerase II beta levels are a determinant of melphalan-induced DNA crosslinks and sensitivity to cell death. *Biochemical Pharmacology*, 72(1), 11–18. <http://doi.org/10.1016/j.bcp.2006.03.017>

Etienne-Manneville, S. (2008). Polarity proteins in migration and invasion. *Oncogene*, 27(55), 6970–6980. <http://doi.org/10.1038/onc.2008.347>

Gallego-Muñoz, P., Ibares-Frías, L., Valsero-Blanco, M. C., Cantalapiedra-Rodriguez, R., Merayo-Llodes, J., & Martínez-García, M. C. (2017). Effects of TGF $\beta$ , PDGF-BB, and bFGF, on human corneal fibroblasts proliferation and differentiation during stromal repair. *Cytokine*, 96, 94–101. <http://doi.org/10.1016/j.cyto.2017.03.011>

Grue P, Grasser A, Sehested M, Jensen PB, Uhse A, Straub T et al. (1998). Essential mitotic functions of DNA topoisomerase II $\alpha$  are not adopted by topoisomerase II $\beta$  in human H69 cells. *J Biol Chem*; 273: 33660–33666.

Guo, S., DiPietro, L. A. (2010). Factors Affecting Wound Healing. *Journal of Dental Research*, 89(3), 219–229. <http://doi.org/10.1177/0022034509359125>

Gupta, K. P., Swain, U., Rao, K. S., & Kondapi, A. K. (2012). Topoisomerase II $\beta$  regulates base excision repair capacity of neurons. *Base Excision DNA Repair, Brain Function and Ageing* Indo-US Workshop on Base Excision DNA Repair, Brain Function and Ageing, 133(4), 203–213.

Hasinoff, B. B., Creighton, A. M., Kozlowska, H., Thampatty, P., Allan, W. P., and Yalowich, J. C. (1997). Mitindomide is a catalytic inhibitor of DNA topoisomerase II that acts at the bisdioxopiperazine binding site. *Mol. Pharmacol.* 52, 839–845

Hasinoff, B. B., Abram, M. E., Barnabe, N., Khelifa, T., Allan, W. P. & Yalowich, J. C. (2001). The catalytic DNA topoisomerase II inhibitor dexrazoxane (ICRF-187)

induces differentiation and apoptosis in human leukemia K562 cells. *Mol. Pharmacol.* 59, 453–461.

Hassan, H. T., & Zander, A. (1996). Stem cell factor as a survival and growth factor in human normal and malignant hematopoiesis. *Acta Haematologica*, 95(3-4), 257–262.

Heng, X., Jin, G., Zhang, X., Yang, D., Zhu, M., Fu, S., et al. (2012). Nurr1 regulates Top II $\beta$  and functions in axon genesis of mesencephalic dopaminergic neurons. *Molecular Neurodegeneration*, 7(1), 4. <http://doi.org/10.1186/1750-1326-7-4>

Hu, T., Sage, H., Hsieh, T. S. (2002). ATPase Domain of Eukaryotic DNA Topoisomerase II: Inhibition of ATPase activity by the anti-cancer drug bisdioxopiperazine and ATP/ADP-induced dimerization. *Journal of Biological Chemistry*, 277(8), 5944–5951. <http://doi.org/10.1074/jbc.M111394200>

Jamil, S., Mousavizadeh, R., Roshan-Moniri, M., Tebbutt, S. J., McCormack, R. G., Duronio, V., & Scott, A. (2017). Angiopoietin-like 4 Enhances the Proliferation and Migration of Tendon Fibroblasts. *Medicine & Science in Sports & Exercise*, 1–36. <http://doi.org/10.1249/MSS.0000000000001294>

Jensen, P. B., Sorensen, B. S., Demant, E. J., Sehested, M., Jensen, P. S., Vindelov, L., and Hansen, H. H. (1990). Merbarone inhibits the catalytic activity of human topoisomerase II $\alpha$  by blocking DNA cleavage. *Cancer Res.* 50, 3311–3316

Jian-Yong Qian, M. C. Z. L. (2016). Mesenchymal Stromal Cells Promote Axonal Outgrowth Alone and Synergistically with Astrocytes via tPA, 1–16. <http://doi.org/10.1371/journal.pone.0168345>

Ju BG, Lunyak VV, Perissi V, Garcia-Bassets I, Rose DW, Glass CK et al. (2006). A topoisomerase II $\beta$ -mediated dsDNA break required for regulated transcription. *Science*; 312: 1798–1802.

Kalluri, R., Zeisberg, M. (2006). Fibroblasts in cancer. *Nature Reviews Cancer*, 6(5), 392–401. <http://doi.org/10.1038/nrc1877>

Karamichos, D., Lakshman, N., & Petroll, W. M. (2009). An experimental model for assessing fibroblast migration in 3-D collagen matrices. *Cell Motility and the Cytoskeleton*, 66(1), 1–9. <http://doi.org/10.1002/cm.20326>

Lassota, P., Singh, G., and Kramer, R. (1996). Mechanism of Topoisomerase II inhibition by Staurosporine and other protein kinase inhibitors. *J. Biol. Chem.* 271, 26418–26423



Li Y, Hao H, Tzatzalos E, et al. (2014). Topoisomerase IIbeta is required for proper retinal development and survival of postmitotic cells. *Biology Open*. 3(2):172-184. doi:10.1242/bio.20146767.

Linka RM, Porter AC, Volkov A, Mielke C, Boege F, Christensen MO. (2007). C-terminal regions of topoisomerase IIalpha and IIbeta determine isoform-specific functioning of the enzymes in vivo. *Nucleic Acids Res*; 35: 3810–3822

Lombardi, L., Persiconi, I., Gallo, A., Hoogenraad, C. C., & De Stefano, M. E. (2017). NGF-dependent axon growth and regeneration are altered in sympathetic neurons of dystrophic mdx mice. *Molecular and Cellular Neuroscience*, 80, 1–17.

Lu, Y.-Y., Zhao, X.-K., Yu, L., Qi, F., Zhai, B., Gao, C.-Q., & Ding, Q. (2017). Interaction of Src and Alpha-V Integrin Regulates Fibroblast Migration and Modulates Lung Fibrosis in A Preclinical Model of Lung Fibrosis. *Nature Publishing Group*, 1–11. <http://doi.org/10.1038/srep46357>

Lyu Y. L., Wang J. C. (2003). Aberrant lamination in the cerebral cortex of mouse embryos lacking DNA topoisomerase IIbeta. *Proc. Natl. Acad. Sci. USA* 100, 7123–7128 10.1073/pnas.1232376100

Lyu YL, Kerrigan JE, Lin CP, Azarova AM, Tsai YC, Ban Y et al. Topoisomerase IIbeta mediated DNA double-strand breaks: implications in doxorubicin cardiotoxicity and prevention by dexrazoxane. *Cancer Res* 2007; 67: 8839–8846.

Mandraj, R., Chekuri, A., Bhaskar, C., Duning, K., Kremerskothen, J., & Kondapi, A. K. (2011). Topoisomerase II $\beta$  associates with Ku70 and PARP-1 during double strand break repair of DNA in neurons. *Archives of Biochemistry and Biophysics*, 516(2), 128–137. <http://doi.org/10.1016/j.abb.2011.10.001>

Nevin, L. M., Xiao, T., Staub, W. and Baier, H. (2011). Topoisomerase IIbeta is required for lamina-specific targeting of retinal ganglion cell axons and dendrites. *Development* 138, 2457-2465.

Nguyen, T. T. T., Park, W. S., Park, B. O., Kim, C. Y., Oh, Y., Kim, J. M., et al. (2016). PLEKHG3 enhances polarized cell migration by activating actin filaments at the cell front. *Proceedings of the National Academy of Sciences*, 113(36), 10091–10096. <http://doi.org/10.1073/pnas.1604720113>

Nur-E-Kamal A., Meiners S., Ahmed I., Azarova A., Lin C. P., Lyu Y. L., Liu L. F. (2007). Role of DNA topoisomerase IIbeta in neurite outgrowth. *Brain Res*. 1154, 50–60 10.1016/j.brainres.2007.04.029

Nur-E-Kamal, A., Meiners, S., Ahmed, I., Azarova, A., Lin, C. P., Lyu, Y. L. and Liu, L. F. (2007). Role of DNA topoisomerase IIbeta in neurite outgrowth. *Brain Res*. 1154, 50-60.

Park, J., Koito, H., Li, J., & Han, A. (2009). Microfluidic compartmentalized co-culture platform for CNS axon myelination research. *Biomedical Microdevices*, 11(6), 1145–1153. <http://doi.org/10.1007/s10544-009-9331-7>

Petrie, R. J., & Yamada, K. M. (2012). At the leading edge of three-dimensional cell migration. *Journal of Cell Science*, 125(24), 5917–5926. <http://doi.org/10.1242/jcs.093732>

Petrie, R. J., Doyle, A. D., & Yamada, K. M. (2009). Random versus directionally persistent cell migration. *Nature Reviews Molecular Cell Biology*, 10(8), 538–549. <http://doi.org/10.1038/nrm2729>

Pouliot N, Pearson HB, Burrows A. Investigating Metastasis Using In Vitro Platforms. In: *Madame Curie Bioscience Database* [Internet]. Austin (TX): Landes Bioscience; 2000-2013. <https://www.ncbi.nlm.nih.gov/books/NBK100379/>

Roca, J. Ishida, R. BERGER, JM. Andoh, T. Wang, JC.(1994). Antitumor bisdioxopiperazines inhibit yeast DNA topoisomerase II by trapping the enzyme in the form of a closed protein clamp, *Proc. Nati. Acad. Sci. USA*, Vol. 91, pp. 1781-1785

Rodriguez-Menocal, L., Salgado, M., Ford, D., & Van Badiavas, E. (2012). Stimulation of Skin and Wound Fibroblast Migration by Mesenchymal Stem Cells Derived from Normal Donors and Chronic Wound Patients. *STEM CELLS Translational Medicine*, 1(3), 221–229. <http://doi.org/10.5966/sctm.2011-0029>

Samson, A. J., Robertson, G., Zagnoni, M., & Connolly, C. N. (2016). Neuronal networks provide rapid neuroprotection against spreading toxicity. *Nature Publishing Group*, 1–11. <http://doi.org/10.1038/srep33746>

Isik, S., Sano, K., Tsutsui, K., Seki, M., Enomoto, T., Saitoh, H., & Tsutsui, K. (2003). The SUMO pathway is required for selective degradation of DNA topoisomerase IIh induced by a catalytic inhibitor ICRF-193 1. *FEBS Letters*, 546(2-3), 374–378. [http://doi.org/10.1016/S0014-5793\(03\)00637-9](http://doi.org/10.1016/S0014-5793(03)00637-9)

Tan KB, Dorman TE, Falls KM, Chung TD, Mirabelli CK, Crooke ST, Mao J (Jan 1992). "Topoisomerase II alpha and topoisomerase II beta genes: characterization and mapping to human chromosomes 17 and 3, respectively". *Cancer Research*. 52 (1): 231–4. PMID 1309226.

Tanabe, K., Ikegami, Y., Ishida, R., and Andoh, T. (1991). *Cancer Res.* 51, 4903–4908

Tiwari V. K., Burger L., Nikolettou V., Deogracias R., Thakurela S., Wirbelauer C., Kaut J., Terranova R., Hoerner L., Mielke C. et al. (2012). Target

genes of Topoisomerase II $\beta$  regulate neuronal survival and are defined by their chromatin state. *Proc. Natl. Acad. Sci. USA* 109, E934–E943  
10.1073/pnas.1119798109

Trepac, X., Chen, Z., & Jacobson, K. (2012). *Cell Migration* (Vol. 105, pp. 13–46). Hoboken, NJ, USA: John Wiley & Sons, Inc. <http://doi.org/10.1002/cphy.c110012>

Tsutsui, K., Tsutsui, K., Okada, S., Watanabe, M., Shohmori, T., Seki, S. and Inoue, Y. (1993). Molecular cloning of partial cDNAs for rat DNA topoisomerase II isoforms and their differential expression in brain development. *J. Biol. Chem.* 268, 19076-19083.

Vejpongsa P, Yeh ET. Topoisomerase 2beta: a promising molecular target for primary prevention of anthracycline-induced cardiotoxicity. *Clin Pharmacol Ther* 2014; 95: 45–52.

Wang, C.-H., Verma, S., Hsieh, I.-C., Hung, A., Cheng, T.-T., Wang, S.-Y., et al. (2007). Stem cell factor attenuates vascular smooth muscle apoptosis and increases intimal hyperplasia after vascular injury. *Arteriosclerosis, Thrombosis, and Vascular Biology*, 27(3), 540–547.  
<http://doi.org/10.1161/01.ATV.0000257148.01384.7d>

Xiao, H. Mao, Y. Desai, SD. Zhou, N. Ting, CY, Hwang, J. Liu, LF. (2003). The topoisomerase II circular clamp arrests transcription and signals a 26S proteasome pathway. *Cell Biology*, 1–6.

Yan W., Suominen J., Toppaari J. (2000). Stem cell factor protects germ cells from apoptosis in vitro. *Journal of Cell Science* 113, 161–168.

Yanagida, M. & Wang, J. C. (1987) in *Nucleic Acids and Molecular Biology*, eds. Eckstein, F. & Lilley, D. M. J. (Springer, Berlin), Vol. 1, pp. 196-209.

Yang X., Li W., Prescott E. D., Burden S. J., Wang J. C. (2000). DNA topoisomerase IIbeta and neural development. *Science* 287, 131–134  
10.1126/science.287.5450.131

Zhang, S., Liu, X., Bawa-Khalife, T., Lu, L. S., Lyu, Y. L., Liu, L. F. and Yeh, E. T. (2012). Identification of the molecular basis of doxorubicin-induced cardiotoxicity. *Nat. Med.* 18, 1639-1642.